Talanta 124 (2014) 60–66

Contents lists available at ScienceDirect

Talanta

journal homepage: www.elsevier.com/locate/talanta

Ultrasensitive non-mediator electrochemical immunosensors using Au/Ag/Au core/double shell nanoparticles as enzyme-mimetic labels

Yulan Wang, Yong Zhang, Yu Su, Feng Li, Hongmin Ma, He Li, Bin Du, Qin Wei *

Key Laboratory of Chemical Sensing & Analysis in Universities of Shandong, School of Chemistry and Chemical Engineering, University of Jinan, Jinan 250022, PR China

ARTICLE INFO

Article history:
Received 21 November 2013
Received in revised form
17 February 2014
Accepted 18 February 2014
Available online 25 February 2014

Keywords:
Cancer diagnosing
Electrochemical immunosensor
Enzyme-mimetic label
Core/shell nanoparticle
Hydrogen peroxide

ABSTRACT

Determination of squamous cell carcinoma antigen (SCCA) in human serum plays an important role in diagnosis of cervical squamous cell carcinoma. In this work, Au/Ag/Au core/double shell nanoparticles (Au/Ag/Au NPs) were prepared by a simple approach and were used as novel enzyme-mimetic labels for development of a sandwich-type electrochemical immunosensor for SCCA. The nanostructure of Au/Ag/Au NPs could be well confirmed by transmission electron microscope (TEM) and UV–vis spectra. Au NPs decorated mercapto-functionalized graphene sheets (Au@SH-GS) were used as platform for immobilization of primary antibody (Ab_1), while Au/Ag/Au NPs were employed as labels of secondary antibody (Ab_2). Due to the excellent electrocatalytic activity of Au/Ag/Au NPs towards the reduction of hydrogen peroxide (H_2O_2), electrochemical amperometric responses to SCCA were achieved after the immuno-reaction. Under optimum conditions, the electrochemical immunosensor exhibited a wide linear range from 0.5 pg/mL to 40 ng/mL with a low detection limit of 0.18 pg/mL for SCCA. The designed immunosensor displayed an excellent analytical performance with good reproducibility, high selectivity and stability.

1. Introduction

Squamous cell carcinoma antigen (SCCA) is a kind of tumor cell-associated glucoprotein that belongs to the family of serine protease inhibitors and locates in 18q21.3 gene locus. It was originally separated from the uterine cervix by Kato and Torigoe in 1977 [1]. SCCA is a specific and efficient squamous cell carcinoma tumor marker that plays an important role in cancer diagnosis originated in squamous cells [2], especially in diagnosis of cervical squamous cell carcinoma. The detection rate of SCCA is 87.7% before proceeding treatment, which is much higher than other tumor markers such as CYFRA21-1, CEA, CA125, CA19-9 and CA15-3 [3]. The recurrence probability increases threefold with respect to preoperative patients who have high value of SCCA [3]. Monitoring the recurrence of cervical squamous cell carcinoma could also be achieved by measuring the concentration of SCCA in human serum [4,5]. Therefore, a fast, efficient and ultrasensitive electrochemical immunoassay for determination of the SCCA concentration in human serum is expected to have potential application in the field of cervical squamous cell carcinoma clinic diagnosis and prognosis.

Electrochemical immunosensors have gained considerable attentions in many fields especially in clinical diagnosis in recent years [6,7]. They are based on the principle of highly biospecific recognition interactions between antigens and the corresponding antibodies [8]. Compared with other types of immunosensors based on fluorescence, chemiluminescence, surface plasmon resonance and quartz crystal microbalance, electrochemical immunosensors exhibit several significant advantages including high sensitivity, low cost and easy miniaturization [9]. Sandwich-type structure is mostly widely used in the construction of the electrochemical immunosensors [10]. For sandwich-type immunosensors, signal amplification is mainly achieved by coupling different kinds of labels to secondary antibody (Ab_2), such as enzymes [11], metal nanoparticles [12], functional mesoporous materials [13], and nanocomposite materials [14–16]. Horseradish peroxidase (HRP) with high electrocatalytic activity and good stability is the most popular label for electrochemical immunosensors [17]. However, direct electrical communication between the redox sites of enzymes and the electrode is difficult because the redox sites of the enzymes are located deep inside the protein shell [18]. Therefore, high amount of redox mediators are required to facilitate the electron transfer between enzyme and electrode [19,20]. In recent years, a large number of related researches have been conducted in non-mediator and non-enzyme electrochemical immunosensors. Various new types of enzyme-mimetic labels have been used to electrochemical catalyze the reduction of hydrogen peroxide

* Corresponding author. Tel.: +86 531 82765730; fax: +86 531 82765969.
E-mail address: sdjndxwq@163.com (Q. Wei).

http://dx.doi.org/10.1016/j.talanta.2014.02.035
0039-9140

(H_2O_2) and enhance the sensitivity of the immunosensors [7,14,21,22]. A novel enzyme-mimetic label with simple preparation process, excellent electrocatalytic activity, good chemical stability and biocompatibility is urgently needed in the construction of ultrasensitive electrochemical immunosensor.

Metal nanoparticles, especially various forms of Au nanoparticles (Au NPs) and Ag nanoparticles (Ag NPs), have aroused widespread concerns due to their superior electrocatalytic properties towards the reduction of H_2O_2 [23,24]. Au NPs are widely used in fixing antibody due to its good biocompatibility and chemical stability [25,26], but it was reported that the electrocatalytic performance of Au NPs conjugated to secondary antibody ($Au@Ab_2$) is not obvious [27,28]. Compared with Au NPs, Ag NPs exhibit excellent electrocatalytic activity towards the reduction of H_2O_2 [29,30]. However, it was reported that Ag NPs could react with H_2O_2 [31], thus the chemical stability of Ag NPs is unsatisfactory. This problem can be solved by changing the structure of nanoparticles. A second shell of Au was deposited onto the surface Au/Ag core/shell nanoparticles (Au/Ag NPs) by a simple method, and then Au/Ag/Au core/double shell nanoparticles (Au/Ag/Au NPs) were obtained with good electrocatalytic properties. This composite was proved that it retains the advantages of both Au and Ag NPs. Moreover, Au/Ag/Au NPs show good biocompatibility, chemical stability and better electrocatalytic activity towards the reduction of H_2O_2 than Au/Ag NPs. In this work, Au/Ag/Au NPs were firstly used as labels to conjugate with secondary antibody. Compared to enzyme labeling of the secondary antibodies, Au/Ag/Au NPs have some advantages as follows. Firstly, without the participation of redox mediator, the preparation process of the immunosensor is simplified. Secondly, simple synthesis method and little consumption reduce the initial cost. Thirdly, better stability is achieved because the electrocatalytic activity of enzyme will change quickly if the external environment changes. Lastly, Au/Ag/Au NPs can make electron transfer easier than enzyme. In summary, as enzyme-mimetic labels, Au/Ag/Au NPs exhibit much superior performance than enzyme. Using Au/Ag/Au NPs as labels will achieve higher sensitivity and lower detection limit.

The immobilization of primary antibody (Ab_1) is also important for the increase of sensitivity of the immunosensor. Graphene sheet (GS) has attracted great interests with its unique properties including fast electron transportation, high thermal conductivity, excellent mechanical stiffness and good biocompatibility [32]. In this work, mercapto-functionalized graphene sheets (SH-GS) have been prepared to couple with Au NPs by a simple method. Au NPs decorated mercapto-functionalized graphene sheet (Au@SH-GS) has good electron transfer ability, biocompatibility and large specific surface area, which could enhance the loading amounts of antibodies. Greatly amplified sensitivity has been achieved by using Au@SH-GS as platform in this sandwich-type immunosensor.

2. Materials and methods

2.1. Apparatus and reagents

All electrochemical measurements were performed on a CHI760E electrochemical workstation (Huakeputian Technology Beijing Co., Ltd., China). Transmission electron microscope (TEM) images were obtained from a Hitachi H-600 microscope (Japan). Scanning electron microscope (SEM) images and energy dispersive X-ray spectral data (EDX) were obtained using Quanta FEG250 field emission environmental SEM (FEI, United States) operated at 4 KV. UV–vis measurements were carried out using a Lambda 35 UV/Vis Spectrometer (Perkin-Elmer, United States). Fourier transform infrared spectroscopy (FTIR) spectrum was obtained from VERTEX 70 spectrometer (Bruker, Germany).

Human SCCA antibody and human SCCA antigen were purchased from Shanghai Linc-Bio Science Co., Ltd., China. $AuCl_3 \cdot HCl \cdot 4H_2O$ was obtained from Sinopharm Chemical Reagent Shanghai Co., Ltd, China. 3-mercaptopropyl triethoxysilane (MPTES) was purchased from Aladdin Chemical Shanghai Co., Ltd. Phosphate buffered solution (PBS) was used as electrolyte for all electrochemistry measurement. All other reagents were of analytical grade and ultrapure water was used throughout the study.

2.2. Preparation of the Au@SH-GS@Ab_1

Fig. 1A shows the preparation procedure of the Au@SH-GS@Ab_1. Graphene oxide (GO) was synthesized by the modified Hummers method [33]. A ethanol dispersion of GO (1 wt%, 10 mL) was mixed with 0.2 mL of MPTES and heated to 70 °C under stirring for 1.5 h, then 0.1 mL of 80% hydrazine hydrate was added under 95 °C for another 1.5 h. The SH-GS was obtained after dried in vacuum.

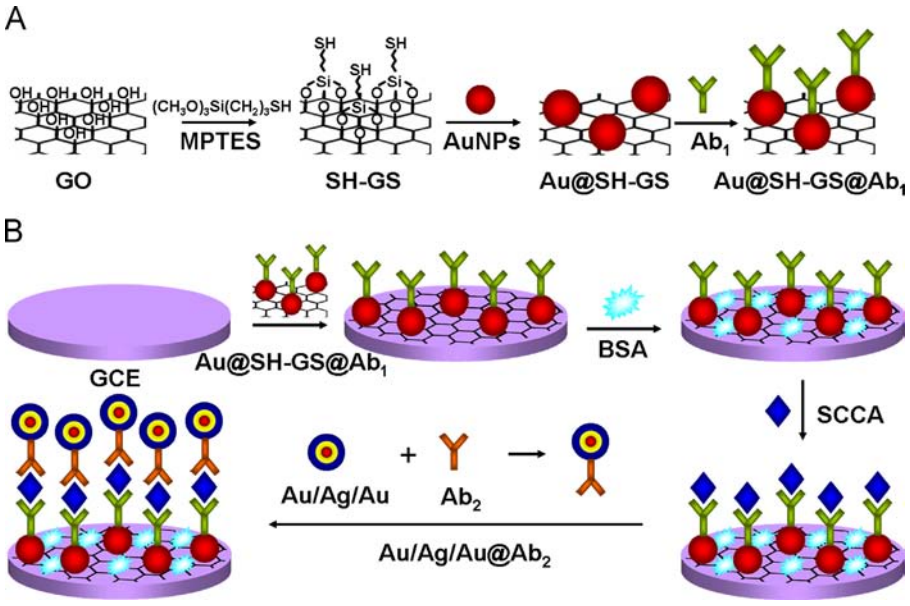

Fig. 1. (A) The preparation procedure of the Au@SH-GS@Ab_1; (B) The schematic illustration of the immunosensor.

Au NPs were synthesized by the classical Frens method [34]. In brief, a solution of $HAuCl_4$ (0.01 wt%, 100 mL) was heated to boiling, and then a solution of trisodium citrate (1 wt%, 2.5 mL) was added. The boiling solution turned a brilliant ruby-red in around 15 min, indicating the formation of monodisperse spherical particles, and then it was cooled to room temperature.

15 mg of SH-GS was mixed with 15 mL of the prepared Au NPs solution under stirring for 12 h, and then Au@SH-GS was obtained by centrifugation and dried at vacuum. A solution of Ab_1 (100 μg/mL, 100 μL) was mixed with Au@SH-GS (2 mg/mL, 1 mL) under stirring for 24 h at 4 °C, followed by centrifugation. The resulting Au@SH-GS@Ab_1 was dispersed in 1 mL of PBS at pH=7.38 and stored at 4 °C until use.

2.3. Preparation of the Au/Ag/Au@Ab_2

Au/Ag/Au NPs were synthesized according to the literature report with minor modifications [35]. First, the Au seeds were prepared according to the method mentioned above. Second, 0.5 mL of 0.1 M ascorbic acid, 0.25 mL of 10 mM $AgNO_3$ and 0.25 mL of Au seeds were added into 10 mL of 50 mM hexadecyl trimethyl ammonium bromide (CTAB) solution, and stirred vigorously with dropwise addition of 60 μL of 1 M NaOH. In this way, the solution turned a bright golden yellow, indicating the Au seeds were coated with first Ag shell. In order to get these particles covered with the second shell of Au, 0.5 mL of 0.1 M ascorbic acid and 164 μL of 1 wt% $HAuCl_4$ were added under vigorous stirring. A dark-blue solution of Au/Ag/Au NPs was obtained.

A solution of Ab_2 (100 μL, 100 μg/mL) was added into 4 mL of prepared Au/Ag/Au NPs solution under stirring for 24 h, followed by centrifugation. The resulting Au/Ag/Au@Ab_2 was dispersed in 1 mL of PBS at pH=7.38 containing 50 mM CTAB and stored at 4 °C until use.

2.4. Fabrication of the immunosensor

Fig. 1B displays the schematic illustration of the immunosensor. A glassy carbon electrode (GCE) with 4 mm diameter was polished to a mirror-like finish with 1.0, 0.3 and 0.05 μm alumina powder and then thoroughly cleaned before use. First, 6 μL of prepared Au@SH-GS@Ab_1 solution was added onto the electrode. After storing at 4 °C for drying, the electrode was incubated in 3 μL of 1 wt% bovine serum albumin (BSA) solution at 4 °C for drying to eliminate nonspecific binding sites. Following that, the electrode was washed thoroughly with PBS at pH=7.38 and incubated with a varying concentration of SCCA for 1 h at room temperature, and then the electrode was washed thoroughly to remove unbounded SCCA. Finally, 6 μL of prepared Au/Ag/Au@Ab_2 solution was added onto the electrode surface for another 1 h at room temperature, then the electrode was washed thoroughly and ready for measurement.

2.5. Detection of SCCA

A conventional three-electrode system was used for all electrochemical measurements: a GCE with 4 mm in diameter as the working electrode, a saturated calomel electrode (SCE) as the reference electrode, and a platinum wire electrode as the counter electrode. The PBS at pH=7.17 was used for all the electrochemical measurements. Cyclic voltammetry was recorded in PBS at 100 mV/s. For amperometric i–t curve to record the amperometric response, a detection potential of −0.4 V was selected. 5 mM H_2O_2 was added into the PBS after the background current was stabilized.

3. Results and discussion

3.1. Characterization of the Au@SH-GS and Au/Ag/Au NPs

Fig. 2A shows the FTIR spectrum of GO (a) and SH-GS (b). O-H stretching of the C-OH at 3420 cm^{-1}, O–H bending of C–OH at 1622 cm^{-1} and C–O vibration of the C–OH at 1232 cm^{-1} prove the existence of hydroxyl group (–OH) in the GO [36]. After chemical reaction, two new peaks appear at around 2920 cm^{-1} and 2850 cm^{-1}, which are assigned to the C–H stretching in the methylene group from MPTES [37]. Another appearing sharp peak with the maximum at 1110 cm^{-1} was identified to be due to the C–O–Si bonding in the SH-GS [37]. The FTIR spectrum proves that the reaction mechanism showed in Fig. 1A is reasonable and the hydrosulfide group (–SH) was successfully connected onto the GS [38]. Fig. 2B and C shows the SEM and TEM of the prepared Au@SH-GS. It could be observed that a large number of Au NPs were successfully attached onto the surface of SH-GS by the interaction between Au NPs and –SH [39]. Fig. 2D shows the EDX picture of the prepared Au@SH-GS. S element in the EDX picture further demonstrated that –SH was connected onto the GS successfully. Au element in the EDX picture indicated that the attached NPs on SH-GS were Au NPs. Al element could be observed because samples were fixed on the aluminum foil to test. And presence of Si element is due to the attached MPTES molecules on Au@SH-GS. TEM image (Fig. 2E) shows the special core/double shell structure of the prepared Au/Ag/Au NPs. Fig. 2F shows the UV–vis spectra and digital photograph of Au (a), Au/Ag (b) and Au/Ag/Au (c) NPs. Different absorption peaks and their subsequent red and blue shifts could confirm the outer shell material [40]. Specifically, the absorption peak and the color of colloidal solution changed depending on the presence of the surface material. The colloidal solution of Au NPs was brilliant ruby-red in color, which shows an absorption peak at 520 nm. When the color of the solution turned to bright golden yellow, Au seed particles were coated with Ag in a further process step. Here, the absorption peak was dominated by Ag and shifted from 520 nm to 430 nm. The following deposition of a second shell of Au, the colloidal solution turned to a dark blue color, which accompanied a complete change of absorption peak from 430 nm to 600 nm. The absorption peak was at approximately 520 nm, 430 nm and 600 nm respectively, which indicated that the prepared NPs were core/shell double structure.

3.2. Optimization of experimental conditions

In order to obtain optimal electrochemical signal, optimization of experimental conditions is necessary. The concentration of Au@SH-GS is an essential factor because it plays an important role in enhancing the electron transfer and immobilization of Ab_1, both of which will affect the amperometric response. Fig. 3A shows the curve of different oxidation peak currents of cyclic voltammograms when the bare GCE was modified with different concentrations of Au@SH-GS in 5 mM potassium ferricyanide solution. As shown in this figure, the optimal amperometric response was achieved at a concentration of 2 mg/mL.

In addition, the amperometric response of the measuring system is related to the pH value of the PBS. The value of pH mainly influences the electrocatalytic process towards the reduction of H_2O_2 and the activity of biological materials. Fig. 3B shows the amperometric response of the immunosensor in different pH values of PBS. As shown in this figure, the optimal amperometric response was achieved at pH=7.17. Therefore, PBS at pH=7.17 was selected for the test throughout this study.

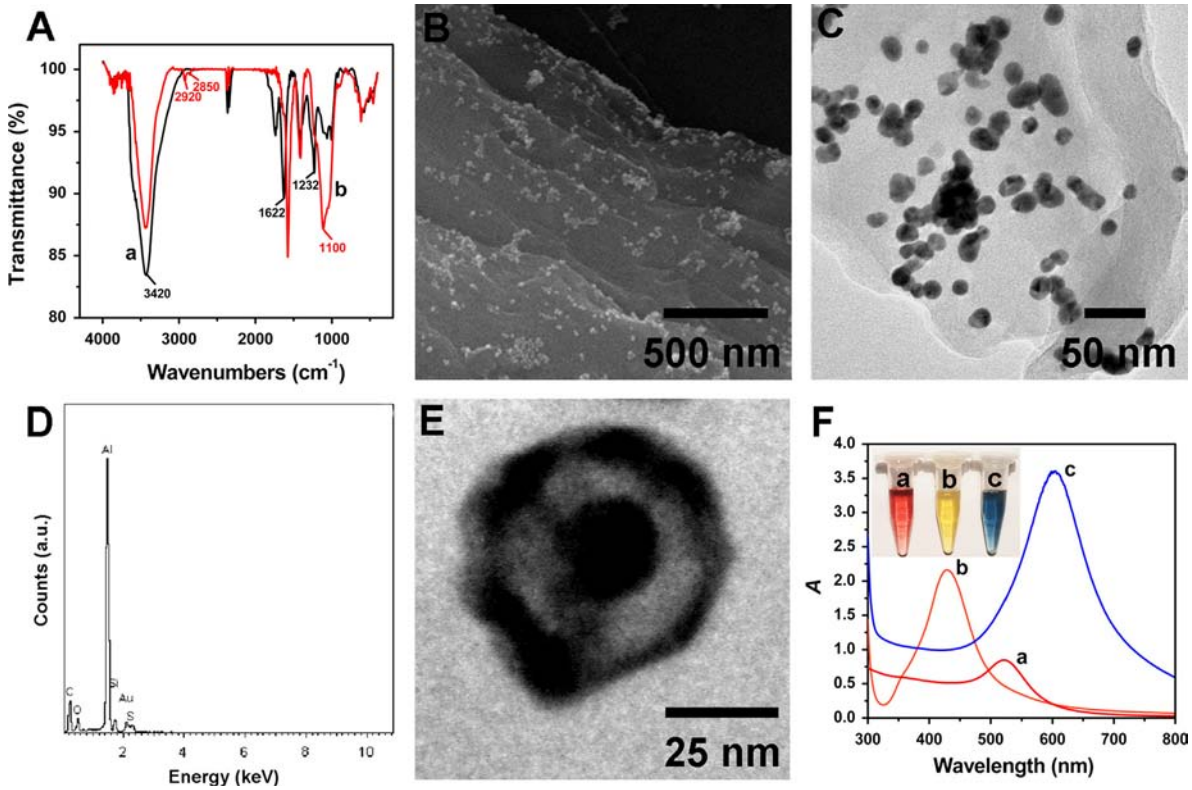

Fig. 2. (A) FTIR spectrum of GO (a) and SH-GS (b); (B) SEM image of Au@SH-GS; (C) TEM image of Au@SH-GS; (D) EDX image of Au@SH-GS; (E) TEM image of Au/Ag/Au NPs; (F) UV–vis spectra and digital photograph of Au (a), Au/Ag (b) and Au/Ag/Au (c) NPs.

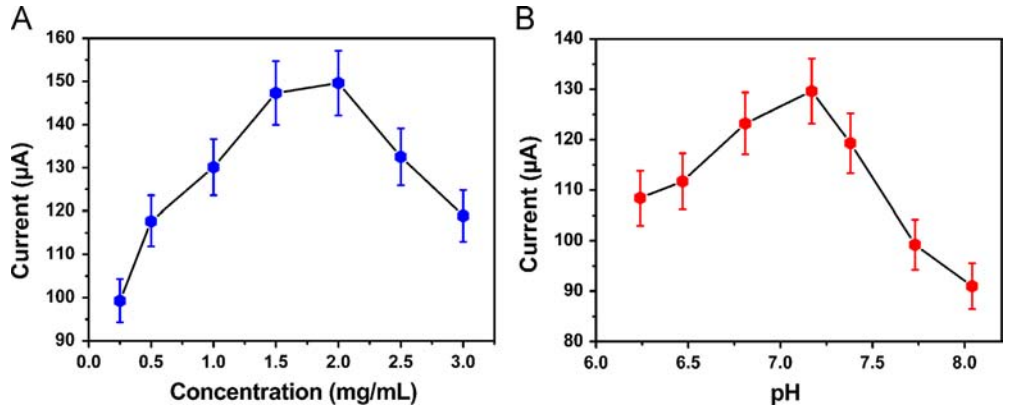

Fig. 3. (A) Amperometric response of bare GCE modified with different concentrations of Au@SH-GS in 5 mM potassium ferricyanide solution; (B) Amperometric response of the immunosensor of 10 ng/mL SCCA towards the reduction of 5 mM H_2O_2 in different pH values of PBS. Error bar=RSD (n=5).

3.3. Characterization of the immunosensor

In this study, cyclic voltammetry was used to study the electron transfer ability of Au@SH-GS. Fig. 4A(a) shows the cyclic voltammogram of bare GCE in 5 mM potassium ferricyanide solution, and Fig. 4A(b) shows the cyclic voltammogram of bare GCE modified with 2 mg/mL Au@SH-GS in 5 mM potassium ferricyanide solution. By comparison, a significantly increasing of amperometric response could be clearly observed. It indicated that the Au@SH-GS could amplify the electrochemical signal, enhance the electron transfer and improve the sensitivity.

In this study, the AC impedance method was used to characterize the assembly process of the electrode. Fig. 4B shows the Nyquist plots of AC impedance spectroscopy in the process of modifying electrode. Nyquist plots are consist of two portions. The linear portion at low frequencies is associated with electrochemical behavior limited by diffusion. The semicircle portion at high frequencies is associated with the electrochemical process subject to electron transfer, where the diameter corresponds to the resistance. Simply, resistance change could be judged by observing the diameter change of semicircle portion. Thus, AC impedance is a suitable method for monitoring the changes in the surface features during the assembly process. In this work, Au@SH-GS@Ab_1 (b), BSA (c) and SCCA (d) were modified layer by layer on the bare GCE (a). The gradually increased resistance indicated the successful modification. Au/Ag/Au@Ab_2 (e) was modified on the electrode, and an obvious decrease of resistance could be observed by comparing curve d with curve e. The electron transfer ability of

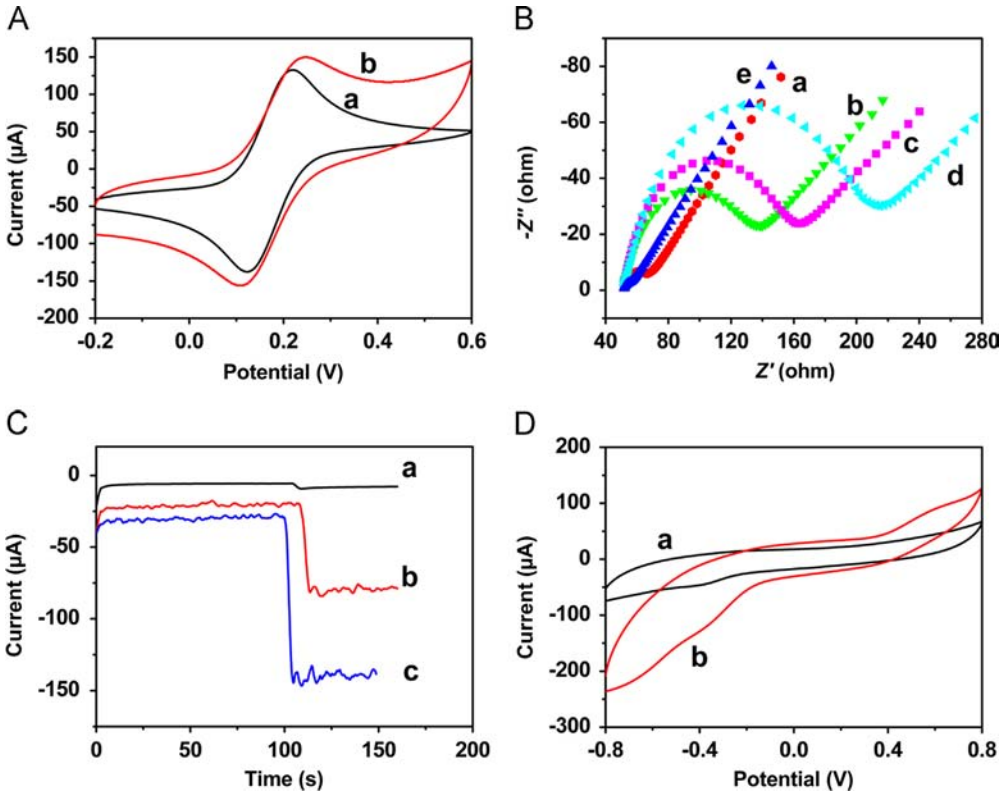

Fig. 4. (A) Cyclic voltammograms of bare GCE modified without (a) and with (b) 2mg/mL Au@SH-GS in 5 mM potassium ferricyanide solution; (B) Nyquist plots of the AC impedance for each immobilized step recorded from 1 to 10^5 Hz of bare GCE (a), Au@SH-GS@Ab_1/GCE (b), BSA/Au@SH-GS@Ab_1/GCE (c), SCCA/BSA/Au@SH-GS@Ab_1/GCE (d) and Au/Ag/Au@Ab_2/SCCA/BSA/Au@SH-GS@Ab_1/GCE (e) in PBS at pH=7.38 containing 0.1 M KCl and 2.5 mM $Fe(CN)_6^{3-}/Fe(CN)_6^{4-}$; (C) Amperometric i-t curves of the immunosensor for the detection of 10 ng/mL SCCA without labels (a), with Au/Ag@Ab_2 (b) and Au/Ag/Au@Ab_2 (c) as labels at −0.4 V towards the reduction of 5 mM H_2O_2 in PBS at pH=7.17; (D) Cyclic voltammograms of Au/Ag/Au@Ab_2 modified electrode in PBS at pH=7.17 before (a) and after (b) the addition of 5 mM H_2O_2.

modified electrode was determined by the conductive NPs and non-conductive bioactive substances together. In this case, it is inferred that the electron transfer ability of Au/Ag/Au NPs play a leading role in enhancing the electrochemical signal [41].

In this study, amperometric i–t curve was used to investigate the electrocatalytic performance of Au@SH-GS (Fig. 4C). By comparing curves a and c, Au@SH-GS (a) also has electrocatalytic activity to H_2O_2, but it is rather weaker than Au/Ag/Au NPs (c). Therefore, the electrocatalytic current of Au@SH-GS could be ignored because of the excellent electrocatalytic activity of Au/Ag/Au NPs.

Immunosensors using Au/Ag@Ab_2 as labels were also prepared and characterized. During the immunosensor preparation process, 10 ng/mL SCCA was used in order to compare the electrocatalytic performance of the two different types of labels. The judgment was based on the amperometric response change of the immunosensor towards the reduction of 5 mM H_2O_2. As expected, the immunosensor using Au/Ag/Au@Ab_2 (c) as labels displayed much higher amperometric change, which was about two times of Au/Ag@Ab_2 (b). The high sensitivity could mainly be ascribed to the special core/double shell structure of Au/Ag/Au NPs. Au/Ag/Au NPs not only exhibit good electrocatalytic activity and sensitivity similar to Ag NPs, but also have high chemical stability and biocompatibility similar to Au NPs.

Fig. 4D displays the cyclic voltammogram of the immunosensor for the detection of 10 ng/mL SCCA using Au/Ag/Au@Ab_2 as labels in PBS at pH=7.17 before (a) and after (b) the addition of 5mM H_2O_2. After the addition of H_2O_2, a dramatic increase of the reduction current was observed, demonstrating the good electrocatalytic performance of Au/Ag/Au NPs towards the reduction of H_2O_2 and the high sensitivity of the immunosensor. According to the literature [23,42], the mechanism for H_2O_2 electro-reduction could be expressed as following:

$$H_2O_2 + e^- \rightarrow OH_{ad} + OH^- \quad (1)$$

$$OH_{ad} + e^- \rightarrow OH^- \quad (2)$$

$$2OH^- + 2H^+ \rightarrow 2H_2O \quad (3)$$

Immunosensors using Au/Ag/Au@Ab_2 as labels were used to detect different concentrations of SCCA in PBS at pH=7.17 at −0.4 V under the optimum conditions. The relationship between the amperometric response towards the reduction of 5 mM H_2O_2 and SCCA concentration is showed in Fig. 5. Experimental results showed that the amperometric response change increased linearly with the logarithmic values of the SCCA concentration within the range of 0.5 pg/mL∼40 ng/mL, and with a low limit of 0.18 pg/mL based on S/N=3. And the equation of the calibration curve: $I=97.70+25.33\log C$, $r=0.9880$. Compared with the detection limit for a microtiter plate-based ELISA (0.3 ng/mL), magneto-controlled electrochemical immunosensor (1.0 pg/mL) and other SCCA immunoassay (15.3 pg/mL) [22,39,43], the proposed immunosensor (0.18 pg/mL) has lower detection limit. The low detection limit was attributed to large specific surface area of Au@SH-GS which firmly conjugated with a relatively large amount of Ab_1 and good electrocatalytic activity, chemical stability and biocompatibility of Au/Ag/Au NPs.

3.4. Reproducibility, selectivity and stability

To evaluate the reproducibility of the immunosensor, five electrodes were prepared for the detection of 10 ng/mL SCCA.

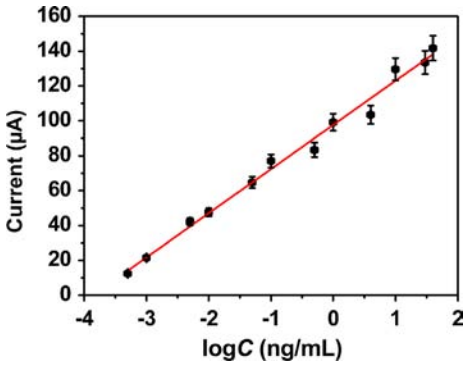

Fig. 5. Calibration curve of the immunosensor towards different concentrations of SCCA. Error bar=RSD (n=5).

Table 1
Determination of SCCA in human serum sample.

Initial SCCA concentration in sample (ng/mL)	Added SCCA concentration (ng/mL)	Measured concentration after addition (ng/mL)	RSD (%, n=5)	Recovery (%, n=5)
1.02	1.00	2.03, 1.98, 1.95, 2.04, 2.07	2.40	99.4
	5.00	5.89, 6.01, 6.12, 5.95, 6.08	1.56	99.8
	10.00	11.09, 11.12, 10.97, 10.88, 11.19	1.12	100.3

Table 2
Human serum sample analysis using the proposed method and the ELISA method.

Sample	This method (ng/mL) [a]	ELISA (ng/mL) [a]	RSD (%)
1	1.14	1.09	−4.59
2	5.32	5.12	−3.91
3	10.04	10.47	4.11
4	20.33	19.81	−2.62
5	40.50	42.10	3.80

[a] each value is the average of five measurements.

The relative standard deviation (RSD) of the measurements was 2.09%, suggesting the reproducibility of the proposed immunosensor was quite good.

To investigate the specificity of the fabricated immunosensor, interferences study was performed using vitamin C, BSA, glucose and alpha fetoprotein (AFP). The 1 ng/mL SCCA solution containing 100 ng/mL interfering substances was measured by the immunosensor. The current variation due to the interfering substances was less than 5% of that without interferences, indicating the selectivity of the proposed immunosensor was acceptable.

To test the stability of the immunosensor, the sensor was stored at 4 °C when not in use. After two weeks, no apparent current change was found. The good stability can be ascribed to the good chemical stability and biocompatibility of Au@SH-GS and Au/Ag/Au NPs. The reproducibility, selectivity and stability of this immunosensor was acceptable, thus it was suitable for the determination of SCCA in real samples.

3.5. Real sample analysis

In order to test the precision and accuracy of the proposed immunosensor, it was used to detect the recoveries of different concentrations of SCCA in human serum sample by standard addition methods (Table 1). The RSD was in the range from 1.12% to 2.40% and the recovery was in the range from 99.4% to 100.3%. Thus, the proposed immunosensor could be effectively applied to the determination of SCCA in human serum.

In order to further validate the proposed immunosensor, a comparison with the commercialized available enzyme-linked immunosorbent assay (ELISA) method is shown in Table 2. The RSD between two methods was in the range from −4.59% to 4.11%. These data revealed a good agreement between the both analytical methods, further indicating the feasibility of the proposed immunosensor for clinical application.

4. Conclusions

This work has developed a novel immunosensor using the Au/Ag/Au NPs as labels for SCCA detection. The immunosensor was prepared based on a sandwich-type protocol with Au@SH-GS as platform. The immunosensor using the Au/Ag/Au NPs as labels displayed a linear response for the detection of SCCA within a wide range (0.5 pg/mL∼40 ng/mL). The proposed immunosensor showed low detection limit (0.18 pg/mL), good reproducibility, high selectivity and acceptable stability. The simple fabrication procedure plus the ultrasensitivity demonstrated by the immunosensor may provide wide potential applications for the detection of SCCA in clinical diagnosis.

Acknowledgments

This study was supported by the Natural Science Foundation of China (Nos. 21175057, 21375047 and 21377046), the National Undergraduate Innovative Training Program of China (No. 201210427024), the Science and Technology Plan Project of Jinan (No. 201307010) and QW thanks the Special Foundation for Taishan Scholar Professorship of Shandong Province and UJN (No.ts20130937).

References

[1] H. Kato, T. Torigoe, Cancer 40 (1977) 1621–1628.
[2] J. van de Lande, E.M. Davelaar, S. von Mensdorff-Pouilly, T.J. Water, J. Berkhof, W.M. van Baal, P. Kenemans, R.H. Verheijen, Gynecol. Oncol. 112 (2009) 119–125.
[3] M.J. Duffy, Ann. Clin. Biochem. 41 (2004) 370–377.
[4] F. Forni, G. Ferrandina, F. Deodato, G. Macchia, A.G. Morganti, D. Smaniotto, S. Luzi, G. D'Agostino, V. Valentini, N. Cellini, Int. J. Radiat. Oncol. Biol. Phys. 69 (2007) 1145–1149.
[5] G. Ferrandina, G. Macchia, F. Legge, F. Deodato, F. Forni, C. Digesù, V. Carone, A.G. Morganti, G. Scambia, Oncology 74 (2008) 42–49.
[6] Y. Cai, H. Li, Y. Li, Y. Zhao, H. Ma, B. Zhu, C. Xu, Q. Wei, D. Wu, B. Du, Biosens. Bioelectron. 36 (2012) 6–11.
[7] R. Feng, Y. Zhang, H. Ma, D. Wu, H. Fan, H. Wang, H. Li, B. Du, Q. Wei, Electrochim. Acta 97 (2013) 105–111.
[8] J.H. Jung, D.S. Cheon, F. Liu, K.B. Lee, T.S. Seo, Angew. Chem. Int. Ed. 49 (2010) 5708–5711.
[9] M. Yang, H. Li, A. Javadi, S. Gong, Biomaterials 31 (2010) 3281–3286.
[10] L. Wang, J. Lei, R. Ma, H. Ju, Anal. Chem. 85 (2013) 6505–6510.
[11] J. Lin, H. Ju, Biosens. Bioelectron. 20 (2005) 1461–1470.
[12] G. Lai, F. Yan, J. Wu, C. Leng, H. Ju, Anal. Chem. 83 (2011) 2726–2732.
[13] Q. Wei, X. Xin, B. Du, D. Wu, Y. Han, Y. Zhao, Y. Cai, R. Li, M. Yang, H. Li, Biosens. Bioelectron. 26 (2010) 723–729.
[14] Q. Wei, T. Li, G. Wang, H. Li, Z. Qian, M. Yang, Biomaterials 31 (2010) 7332–7339.
[15] Y. Li, Z. Zhong, Y. Chai, Z. Song, Y. Zhuo, H. Su, S. Liu, D. Wang, R. Yuan, Chem. Commun. 48 (2012) 537–539.
[16] N. Liu, X. Chen, Z. Ma, Biosens. Bioelectron. 48 (2013) 33–38.
[17] J. Tang, D. Tang, B. Su, Q. Li, B. Qiu, G. Chen, Electrochim. Acta 56 (2011) 8168–8175.
[18] C. Ruan, F. Yang, C. Lei, J. Deng, Anal. Chem. 70 (1998) 1721–1725.
[19] Y. Dai, Y. Cai, Y. Zhao, D. Wu, B. Liu, R. Li, M. Yang, Q. Wei, B. Du, H. Li, Biosens. Bioelectron. 28 (2011) 112–116.
[20] Q. Wei, R. Li, B. Du, D. Wu, Y. Han, Y. Cai, Y. Zhao, X. Xin, H. Li, M. Yang, Sens. Actuators, B 153 (2011) 256–260.
[21] Q. Wei, Y. Zhao, B. Du, D. Wu, Y. Cai, K. Mao, H. Li, C. Xu, Adv. Funct. Mater. 21 (2011) 4193–4198.

[22] D. Wu, H. Fan, Y. Li, Y. Zhang, H. Liang, Q. Wei, Biosens. Bioelectron. 46 (2013) 91–96.
[23] F. Meng, X. Yan, J. Liu, J. Gu, Z. Zou, Electrochim. Acta 56 (2011) 4657–4662.
[24] E. Kurowska, A. Brzózka, M. Jarosz, G.D. Sulka, M. Jaskuła, Electrochim. Acta 104 (2013) 439–447.
[25] Y. Cao, R. Yuan, Y. Chai, L. Mao, H. Niu, H. Liu, Y. Zhuo, Biosens. Bioelectron. 31 (2012) 305–309.
[26] H. Zhang, L. Liu, X. Fu, Z. Zhu, Biosens. Bioelectron. 42 (2013) 23–30.
[27] Q. Wei, Z. Xiang, J. He, G. Wang, H. Li, Z. Qian, M. Yang, Biosens. Bioelectron. 26 (2010) 627–631.
[28] A. Guo, D. Wu, H. Ma, Y. Zhang, H. Li, B. Du, Q. Wei, J. Mater. Chem. B 1 (2013) 4052–4058.
[29] W. Zhao, H. Wang, X. Qin, X. Wang, Z. Zhao, Z. Miao, L. Chen, M. Shan, Y. Fang, Q. Chen, Talanta 80 (2009) 1029–1033.
[30] X. Qin, Y. Luo, W. Lu, G. Chang, A.M. Asiri, A.O. Al-Youbi, X. Sun, Electrochim. Acta 79 (2012) 46–51.
[31] G.-L. Wang, X.-Y. Zhu, H.-J. Jiao, Y.-M. Dong, X.-M. Wu, Z.-J. Li, Anal. Chim. Acta 747 (2012) 92–98.
[32] H. Chen, M.B. Müller, K.J. Gilmore, G.G. Wallace, D. Li, Adv. Mater. 20 (2008) 3557–3561.
[33] D.C. Marcano, D.V. Kosynkin, J.M. Berlin, A. Sinitskii, Z. Sun, A. Slesarev, L. B. Alemany, W. Lu, J.M. Tour, ACS Nano 4 (2010) 4806–4814.
[34] G. Frens, Nature 241 (1973) 20–22.
[35] A. Knauer, A. Thete, S. Li, H. Romanus, A. Csaki, W. Fritzsche, J. Köhler, Chem. Eng. J. 166 (2011) 1164–1169.
[36] J. Ou, J. Wang, S. Liu, B. Mu, J. Ren, H. Wang, S. Yang, Langmuir 26 (2010) 15830–15836.
[37] Y. Zhang, Y. Zhu, G. Lin, R.S. Ruoff, N. Hu, D.W. Schaefer, J.E. Mark, Polymer 54 (2013) 3605–3611.
[38] H. Zhu, M. Du, M. Zhang, P. Wang, S. Bao, M. Zou, Y. Fu, J. Yao, Biosens. Bioelectron. 54 (2014) 91–101.
[39] Q. Li, D. Tang, J. Tang, B. Su, G. Chen, M. Wei, Biosens. Bioelectron. 27 (2011) 153–159.
[40] B. Rodriguez-Gonzalez, A. Burrows, M. Watanabe, C.J. Kiely, L.M. Liz Marzan, J. Mater. Chem. 15 (2005) 1755–1759.
[41] S. Du, Z. Guo, B. Chen, Y. Sha, X. Jiang, X. Li, N. Gan, S. Wang, Biosens. Bioelectron. 53 (2014) 135–141.
[42] Y. Zhou, G. Yu, F. Chang, B. Hu, C.-J. Zhong, Anal. Chim. Acta 757 (2012) 56–62.
[43] J.A. Erickson, J. Lu, J.J. Smith, J.A. Bornhorst, D.G. Grenache, E.R. Ashwood, Clin. Chem. 56 (2010) 1496–1499.